

# Effect of mesoporous FA-SiO<sub>2</sub> extracted from fly ash on the structural and photocatalytic properties of g- C<sub>3</sub>N<sub>4</sub>-based materials

Xianhua LI, Qingbo YU

Cite this as: Xianhua LI, Qingbo YU, 2025. Effect of mesoporous FA-SiO<sub>2</sub> extracted from fly ash on the structural and photocatalytic properties of g-C<sub>3</sub>N<sub>4</sub>-based materials. *Journal of Zhejiang University-SCIENCE A (Applied Physics & Engineering)*, 26(7):694-706. <https://doi.org/10.1631/jzus.A2400308>

# Study on the structure of precursor

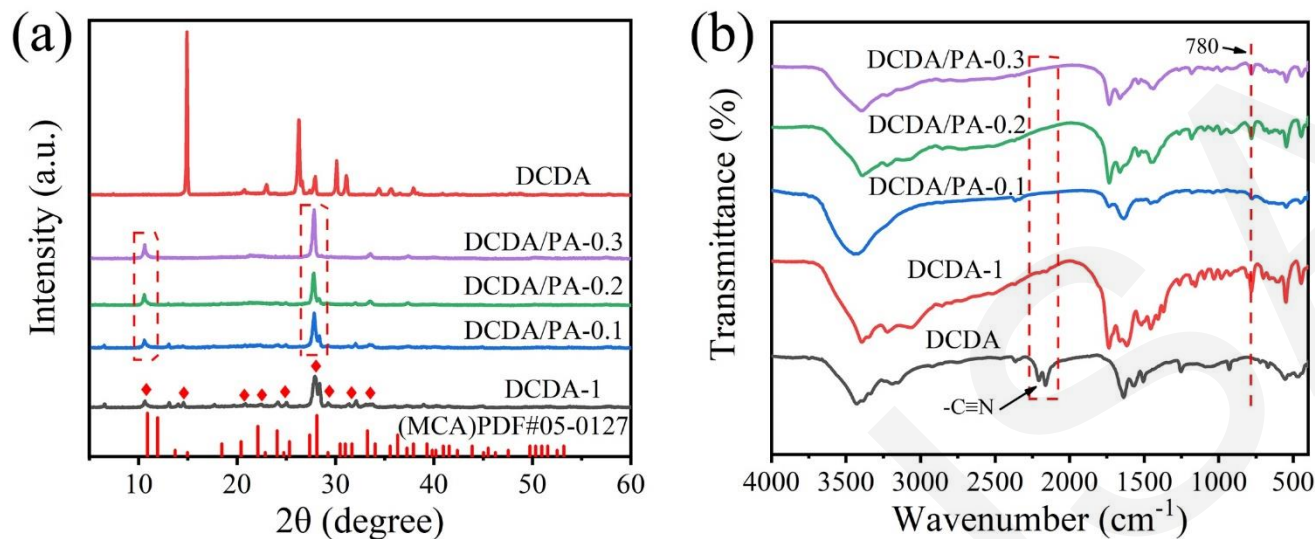


Figure 1 (a) XRD pattern and (b) FT-IR pattern of DCDA, DCDA-1, and DCDA/PA- XX.

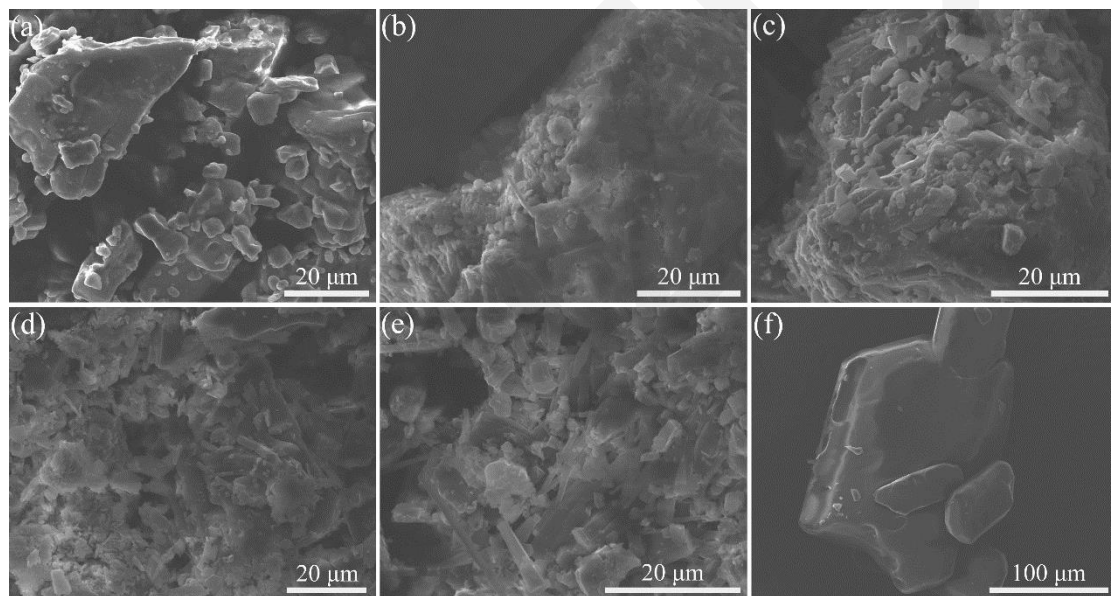


Figure 2 SEM images of (a) DCDA, (b) DCDA-1, (c) DCDA/PA-0.1, (d) DCDA/PA-0.2, (e) DCDA/PA-0.3 and (f) PA.

# Study on the structure of target catalyst

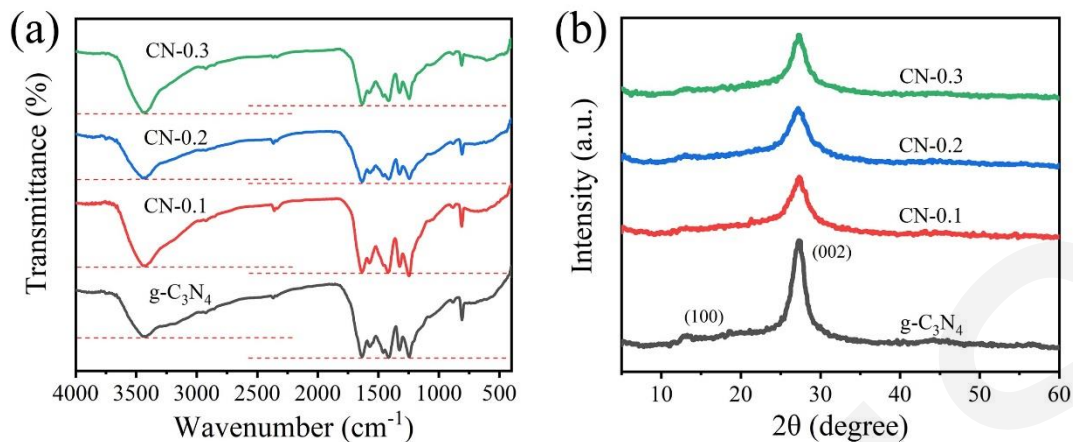


Figure 4 (a) FT-IR and (b) XRD images of  $\text{g-C}_3\text{N}_4$  and CN-X.

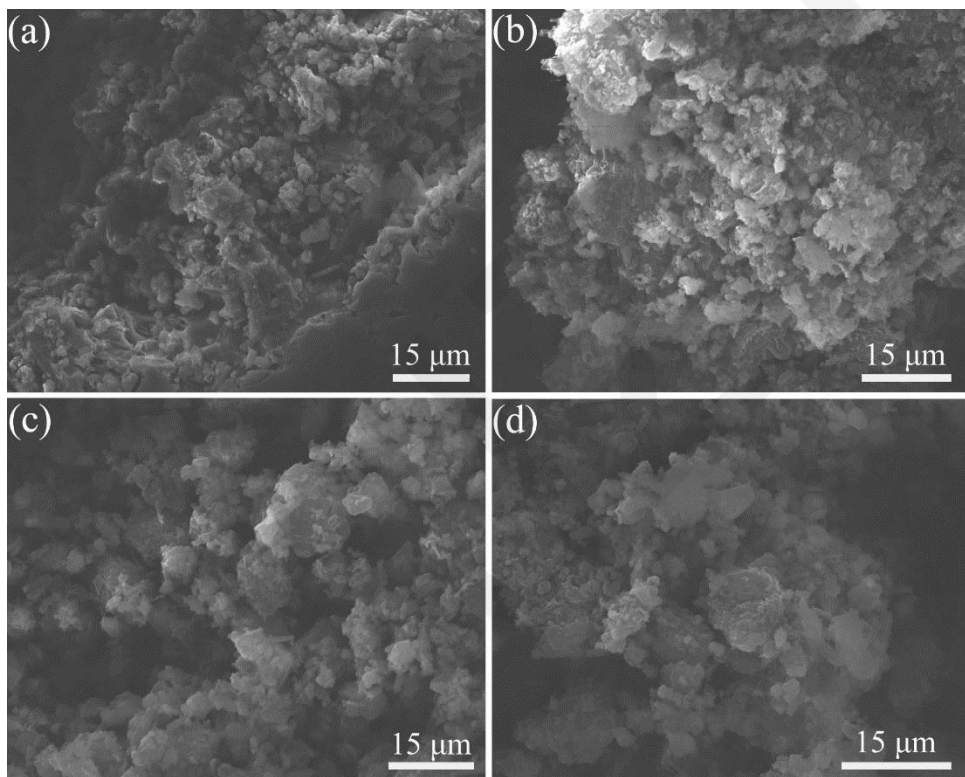


Figure 5 SEM images of (a)  $\text{g-C}_3\text{N}_4$ , (b) CN-0.1, (c) CN-0.2, and (d) CN-0.3.

# Study on thermal decomposition kinetics

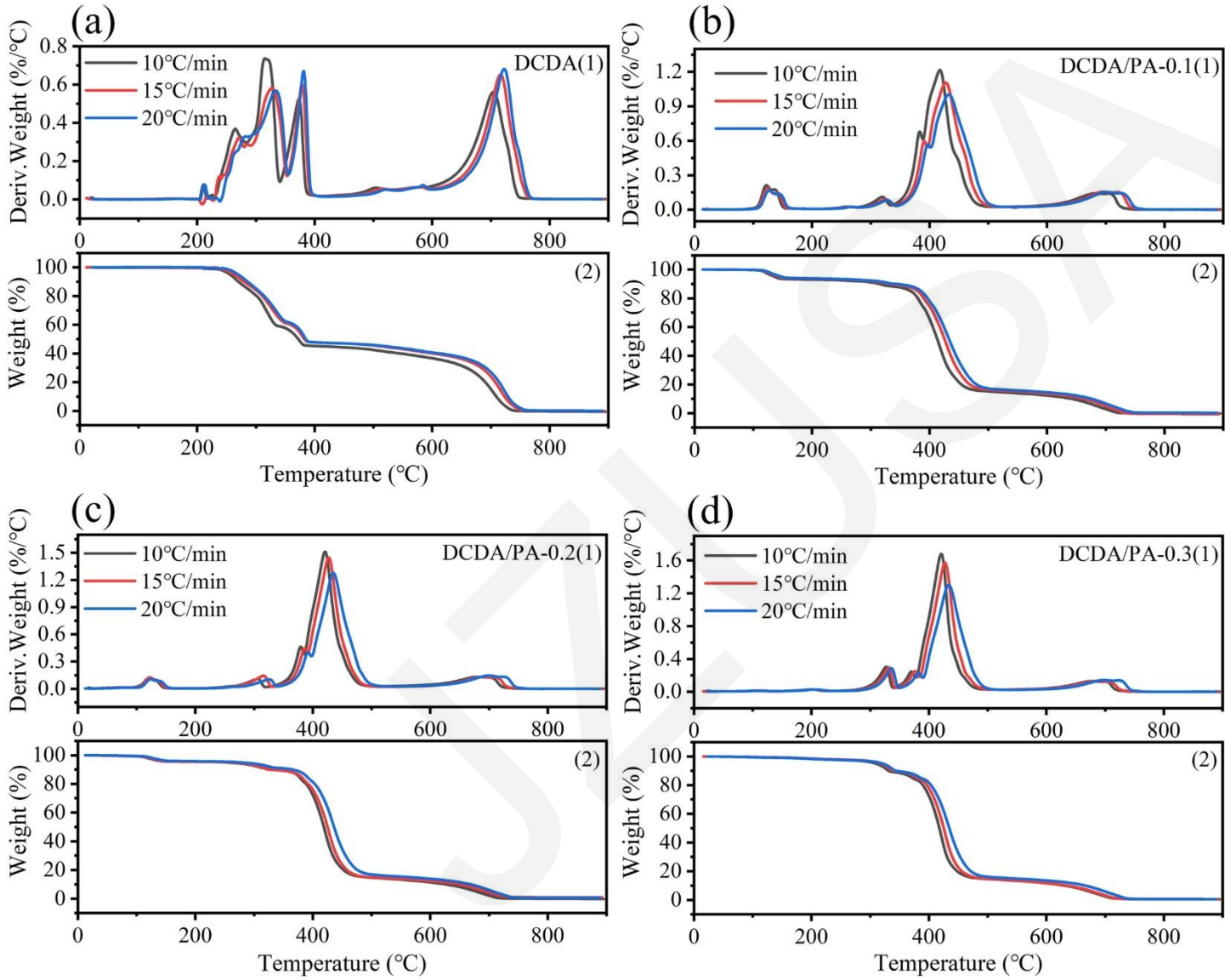


Figure 6 TG-DTG curves of (a) DCDA; (b) DCDA/PA-0.1; (c) DCDA/PA-0.2; (d) DCDA/PA-0.3 ((1): DTG curves; (2): TG curves).

# Study on thermal decomposition kinetics

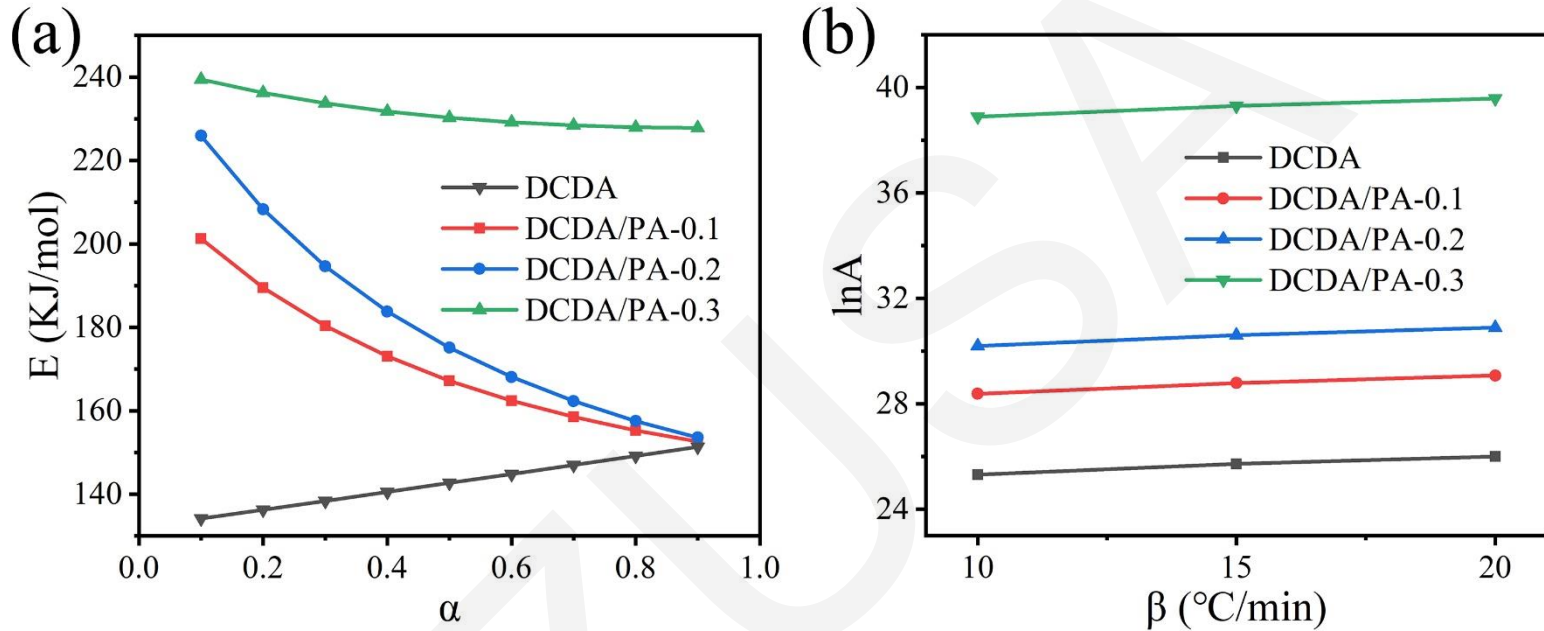


Figure 7 The relationship between (a) activation energy (E) and conversion rate ( $\alpha$ ) of DCDA and DCDA/PA-X; (b) The relationship between the pre-exponential factor (A) and the heating rate ( $\beta$ ).

# Study on photocatalytic performance and mechanism

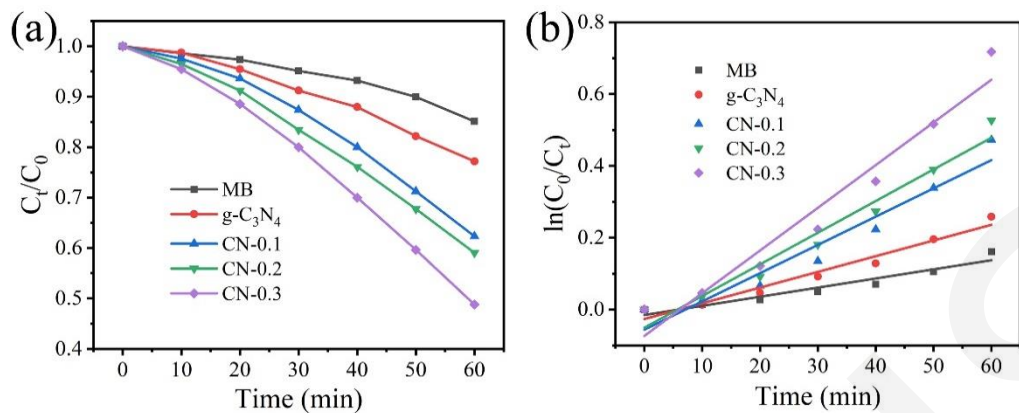


Figure 8 (a) Photocatalytic degradation curves of different samples and (b) Kinetic fitting curve

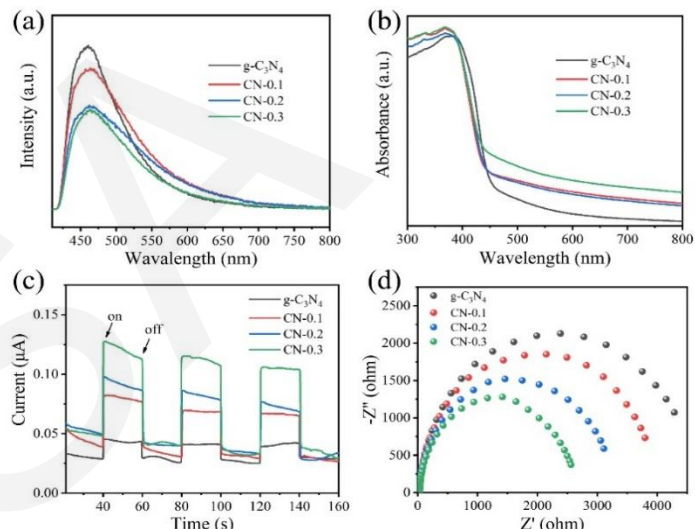


Figure 9 (a) PL spectra of different samples; (b) UV-VIS diffuse reflection spectrum; (c) transient photocurrent and (d) Electrochemical Impedance Spectroscopy.

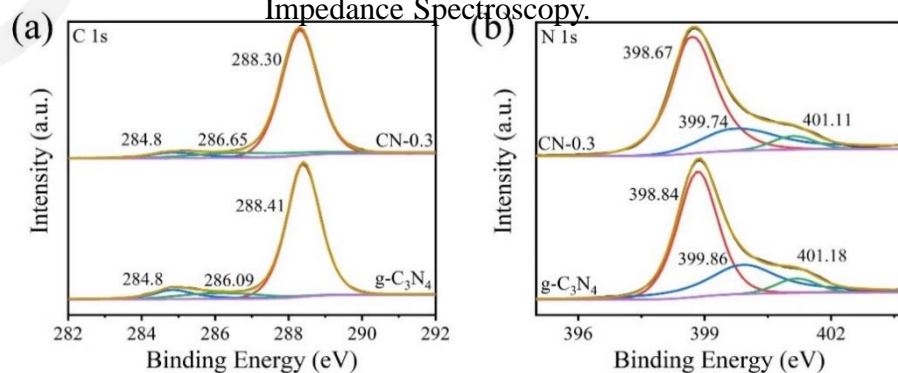
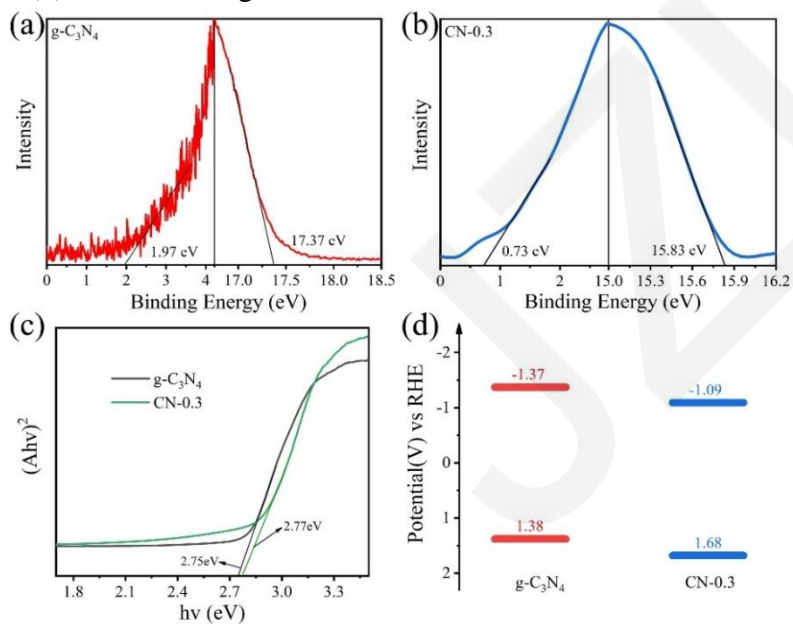


Figure 10 XPS spectra of (a) C 1s and (b) N 1s for  $g-C_3N_4$  and CN-0.3.

Figure 11 Ultraviolet photoelectron spectra of (a)  $g-C_3N_4$  and (b) CN-0.3; (c) Kubelka Munk plots of different samples; (d) Energy level structure diagrams.

# Conclusions

In this chapter, DCDA/PA-0.3 precursor with MCA assembler structure, in which some of the amino groups were bound by phthalic acid through hydrogen bonding interactions, was prepared by hydrothermal treatment of the mixture of dicyanodiamine and phthalic acid, and CN-0.3 photocatalysts were further prepared by heat-shrinking method. The results showed that the assembled structure formed by hydrogen bonding interactions could hinder the intermolecular collision chances during the calcination process of DCDA/PA-0.3 precursor, which made the polymerization reaction difficult to proceed. Finally, an irregular lamellar stacking structure was formed in CN-0.3 photocatalysts. In addition, the CN-0.3 still maintains the characteristic molecular structure of the carbon nitride in the graphite phase and has a higher photogenerated charge carrier separation efficiency than that of the pristine g-C<sub>3</sub>N<sub>4</sub>, which makes CN-0.3 exhibit better visible photocatalytic activity. After simulated visible light irradiation for 60 min, the photocatalytic activity of CN-0.3 for MB was 2.72 times higher than that of the pristine g-C<sub>3</sub>N<sub>4</sub>.